HHS Public Access

Author manuscript

Exp Hematol. Author manuscript; available in PMC 2019 September 03.

Published in final edited form as:

Exp Hematol. 2019 February ; 70: 31–41.e1. doi:10.1016/j.exphem.2018.12.003.

MISTRG mice support engraftment and assessment of nonhuman primate hematopoietic stem and progenitor cells

Stefan Radtke[a], **Yan-Yi Chan**[a], **Trisha R. Sippel**[b], **Hans-Peter Kiem**[a,c,d,*], **Anthony Rongvaux**[b,e,*]

[a]Programs in Cell and Gene Therapy, Clinical Research Division, Fred Hutchinson Cancer Research Center, Seattle, WA, 98109

[b]Programs in Immunology, Clinical Research Division, Fred Hutchinson Cancer Research Center, Seattle, WA, 98109

[c]Department of Medicine, University of Washington School of Medicine, Seattle, WA, 98195

[d]Department of Pathology, University of Washington School of Medicine, Seattle, WA, 98195

[e]Department of Immunology, University of Washington School of Medicine, Seattle, WA, 98195

Abstract

Pre-clinical feasibility, safety, and efficacy testing of hematopoietic stem cell (HSC)-mediated gene therapy approaches is commonly performed in large animal models such as nonhuman primates (NHPs). Here we wished to determine whether mouse models would allow engraftment of NHP HSPCs which would enable more facile and less costly evaluation of promising strategies. In this study, we comprehensively tested two mouse strains for the engraftment of NHP $CD34^+$ hematopoietic stem and progenitor cells. No engraftment of NHP HSPCs was observed in NSG mice, whereas the humanized MISTRG model did demonstrate dose-dependent multilineage engraftment of NHP cells in the peripheral blood, bone marrow, spleen, and thymus. Most importantly and closely mimicking the hematopoietic recovery of autologous stem cell transplants in the NHP, only HSC-enriched $CD34^+CD90^+CD45RA^-$ cell fractions did engraft and reconstituted the bone marrow stem cell niche in MISTRG mice. In summary, we here report the first "monkeynized" mouse xenograft model that closely recapitulates the autologous hematopoietic reconstitution in the NHP stem and progenitor cell transplantation and gene therapy model. Availability of this model has the potential to pre-evaluate novel HSC-mediated gene therapy approaches, inform studies in the NHP, and improve the overall outcome of large-animal experiments.

One Sentence Summary

[*]**Co-corresponding Authors: Anthony Rongvaux**; Fred Hutchinson Cancer Research Center, PO Box 19024, M/S D3-100, 1100 Fairview Avenue N, Seattle, WA 98109, Phone: 206.667.7753 / Fax: 206.667.7983 / rongvaux@fredhutch.org, **Hans-Peter Kiem**, Fred Hutchinson Cancer Research Center, PO Box 19024, M/S D1-100, 1100 Fairview Avenue N, Seattle, WA 98109. Phone: 206.667.4425 / Fax: 206.667.6124; hkiem@fredhutch.org, Website: www.fredhutch.org.

Author contributions: SR, AR and HPK designed the study. SR and YYC performed *in vitro* experiments, longitudinal mouse follow-up, necropsy and data analysis. SR generated the figures. AR and TRS provided mice. AR and HPK funded the study. SR, AR and HPK wrote the manuscript. All authors reviewed and edited the final manuscript.

Conflict of interest disclosure

The authors declare that there are *no conflicts of interest.*

Successful multilineage engraftment of nonhuman primate hematopoietic stem and progenitor cells in the MISTRG mouse model.

Keywords

Hematopoietic stem cells; Nonhuman primate xenograft model; MISTRG mouse model

Introduction

Autologous hematopoietic stem cell (HSC) gene therapy/editing is currently one of the most promising treatment strategies for a broad variety of hematological diseases and disorders [1–4]. The transfer of therapeutic genes to repair deficiencies or the delivery of nucleases to edit genes has the potential to cure diseases such as Fanconi anemia, severe-combined immunodeficiency (SCID), HIV/AIDS and hemoglobinopathies [5–8].

Clinical feasibility, safety, and, in particular, engraftment of genetically modified HSCs is commonly tested in nonhuman primates (NHPs) [9, 10]. Benefits of this large animal model include close similarity in size, weight, and physiology to humans; the ability to perform autologous stem cell transplants with full multilineage support; and the opportunity to take frequent peripheral blood (PB) and bone marrow (BM) samples for a comprehensive long-term follow up. Most importantly, cross-reactivity of markers, reagents, and drugs between humans and NHPs permits an easy translation of successfully tested approaches into clinical treatment strategies.

However, studies in NHPs are expensive and require special facilities and trained staff, making high throughput testing of novel strategies difficult. In many cases, only individual and heavily pre-selected approaches are tested in autologous NHP transplants. Unfortunately, pre-selecting treatment strategies based on *ex vivo* experiments and/or human xenograft assays can bear the risk of misinterpretation, lack of translatability, or, in the worst case, lead to failure of long-lasting and expensive large-animal experiments.

The availability of a mouse model that supports xenotransplantation of NHP cells, mimics the multilineage engraftment of hematopoietic stem and progenitor cells (HSPCs) in the autologous setting [11], and enables functional assessment of gene-modified NHP cells would allow comprehensive and cost-efficient high-throughput screening of potential treatment strategies upfront. The ability to screen multiple experimental parameters in a mouse xenograft model would provide the ability to objectively select conditions for further testing in large-animal studies and ultimately improve the outcome of NHP transplantation studies.

We have previously reported successful but low-level engraftment of gene-modified baboon HSPCs in the NOD/SCID mouse model [12]. Although we detected multilineage donor chimerism and gene-marked cells for up to 12 weeks in these mice, the observed pattern of engraftment, the clonal composition, as well as the frequency of gene marking barely resembled the autologous transplant situation in the baboon.

With the aim to establish a “monkeynized” mouse model that provides higher levels of engraftment, better multilineage support, and more closely recapitulates the autologous hematopoietic recovery, we here performed comprehensive engraftment studies of pigtail macaque (PM) and rhesus macaque (RM) $CD34^+$ in two mouse strains, NSG [13] and MISTRG [14]. Similar to xenograft studies of human HSPCs, we assessed the multilineage engraftment potential of NHP cells in various tissues, determined the homing and engraftment of NHP HSPCs into the BM stem cell niche, and titrated the number of SCID-repopulating cells (SRCs). To validate the read-out of this new “monkeynized” mouse model, we further determined the engraftment potential of phenotypically and functionally defined NHP HSPC subsets in analogy to our recently reported study in the NHP [11].

Results

NSG mice do not support engraftment of NHP HSPCs

The NSG mouse model is the most frequently used xenograft assay for human HSPCs [15]. To determine whether NSG mice support multilineage engraftment of PM HSPCs, bulk $CD34^+$ HSPCs from granulocyte-colony stimulating factor (G-CSF)-primed BM aspirates as well as sort-purified $CD34^+$ subsets enriched for HSCs ($CD90^+CD45RA^-$), multipotent progenitors (MPPs: $CD90^-CD45RA^-$), or lympho-myeloid progenitors (LMPs: $CD90^-CD45RA^+$) were individually transplanted into sub-lethally irradiated adult (250 cGy) as well as neonatal NSG (150 cGy) mice [11]. The frequency of NHP $CD45^+$ cells in the PB was tracked longitudinally, and the engraftment of NHP cells in the BM, spleen and thymus determined after 16–20 weeks at necropsy.

NSG mice did not support engraftment of $CD34^+$ cells or sort-purified NHP $CD34^+$ subsets following transplantation in adult or neonatal recipients (Table 1A). Only a single mouse receiving the HSC-enriched cell fraction demonstrated low levels (<0.3%) of $CD45^+$ NHP cells in the PB that was skewed towards the B lymphoid lineage. However, no engraftment of $CD45^+$ cells or NHP HSPCs was observed in the BM or other tissues in this specific mouse.

To determine whether the transplantation of higher numbers of NHP $CD34^+$ cells would result in successful engraftment in NSG mice, we injected up to 1×10^6 NHP $CD34^+$ cells in adult mice and 7.5×10^5 $CD34^+$ cells in neonatal mice (Table 1B). Even the highest cell doses did not lead to detectable engraftment in any tissues. Similarly, engraftment of $CD34^+$ cells from an alternative stem cell source (steady-state bone marrow, ssBM) or the RM was not supported by the NSG mouse model (Table 1C).

Altogether, engraftment, stem cell homing, and multilineage differentiation of PM and RM HSPCs is not supported by the NSG mouse model.

Robust multilineage engraftment of NHP HSPCs in MISTRG mice

In addition to immunodeficiency of the host, successful xeno-transplantation of HSPCs requires inter-species cross-reactivity of the “don’t eat me” signal mediated by the SIRPα/CD47 axis [16]. NSG mice efficiently support human HSPC engraftment because of a genetic polymorphism, stemming from the NOD genetic background, that alters the

glycosylation of the SIRPα protein and renders it cross-reactive with human CD47 [17]. We reasoned that the NOD-derived SIRPα receptor may not be cross-reactive with NHP CD47, but that the SIRPα/CD47 pair may be cross-reactive between humans and NHPs. Indeed, these proteins are highly conserved among primates (Table 2 and Supplementary Table E1). Therefore, we evaluated NHP hematopoiesis following xeno-transplantation in MISTRG recipient mice. In MISTRG mice, the gene encoding human *SIRPA* was knocked-in in the endogenous *Sirpa* locus, resulting in physiological expression of the human SIRPα protein [18, 19]. MISTRG mice also harbor knock-in humanization of several cytokine-encoding genes (*Csf1*, encoding CSF-1 aka M-CSF; *Il3* encoding interleukin-3; *Csf2* encoding GM-CSF; and *Thpo* encoding thrombopoietin) [14]. The absence of these mouse cytokines affects mouse hematopoiesis, resulting in a form of genetic preconditioning that opens the BM niche for transplanted cells. Furthermore, the human cytokines may support the maintenance and differentiation of NHP HSPCs, since most of these cytokines are highly conserved between humans and NHPs (Table 2 and Supplementary Table E1).

We initially sort-purified PM $CD34^+$ cells and injected them intra-hepatically into neonatal pre-conditioned (150 cGy irradiation) MISTRG mice. We longitudinally tracked engraftment of NHP $CD45^+$ cells in the PB starting in week 8, and analyzed tissues 16–24 weeks post-transplant.

In contrast to NSG mice (Table 1), NHP HSPCs successfully engrafted MISTRG mice (Figure 1). Development of phenotypical NHP granulocytes ($CD11b^+CD14^-$), monocytes ($CD11b^+CD14^+$), B cells ($CD20^+$), NK cells ($CD16^+$) and T cells ($CD3^+$, $CD4^+$, $CD8^+$) was detected in the PB, BM, spleen, and thymus of MISTRG mice (Figure 1A,B). In addition, NHP $CD34^+$ cells, as well as phenotypical CD34 subsets enriched for HSCs, MPPs, and LMPs, were detected in the BM of multilineage engrafted MISTRG mice (Figure 1C).

Intrahepatic injection of 1–20 × 10^5 NHP $CD34^+$ cells into MISTRG mice demonstrated dose-dependent multilineage engraftment in the PB, BM, and spleen (Figure 2A–D, Table 3A). Engraftment of NHP T cells in the thymus was dose-independent and showed either full or no chimerism (Figure 2E). Mice receiving >20 × 10^5 NHP $CD34^+$ cells became anemic or demonstrated significant weight loss and were euthanized 8–10 weeks post-transplant. In contrast to human HSPC transplantation in MISTRG [14], the frequency of phenotypical NHP monocytes ($CD11^+CD14^+$ cells) in the PB and spleen was low but remained stable over time. Among lymphoid cells, B cells were gradually replaced by emerging T cells starting at week 12–14 (Supplementary Figure E1A–D).

Healthy mice did undergo planned euthanasia 16–20 weeks post-transplant to analyze multilineage engraftment of NHP cells in different tissues. NHP granulocytes were predominantly found in the BM, monocytes in the BM and spleen, B cells in the spleen, NK cells in the BM and thymus, and T cells in the thymus of engrafted mice (Figures 1B and 2B–E). Most importantly, NHP $CD34^+$ cells were able to home and repopulate the BM stem cell niche harboring a phenotypically distinct HSC-enriched subset as well as downstream progenitors (Figures 1C and 2F). In addition, BM-resident NHP $CD34^+$ cells were capable to give rise to myeloid, erythroid, as well as erythro-myeloid colonies in colony-forming cell (CFC) assays *ex vivo* (Figure 2G).

In summary, the MISTRG mouse model supports the engraftment of NHP CD34$^+$ HSPCs and their multilineage differentiation to immune cell lineages in the PB and tissues. Furthermore, NHP CD34$^+$ cells can home into the BM stem cell niche of MISTRG mice and successfully reconstitute phenotypically distinct CD34$^+$ cell subsets.

NHP CD90$^+$CD45RA$^-$ cell fractions exclusively engraft in MISTRG

The availability of this novel "monkeynized" MISTRG mouse model enabled us to study the engraftment potential of NHP CD34$^+$ subpopulations. Previously performing competitive repopulation experiments of cultured and gene-modified CD34$^+$ subpopulations in the NHP model, we have shown that CD90$^+$CD45RA$^-$ HSC-enriched cell fractions exclusively contain hematopoietic reconstitution potential [11]. To determine the engraftment potential of MPP- and LMP-enriched cell fractions and whether co-administration of committed progenitor cells is required for HSC engraftment, freshly-isolated, sort-purified, and unmanipulated HSC- (I), MPP- (II), and LMP- (III) enriched cell fractions were transplanted into individual neonatal MISTRG mice (Figure 3A).

In agreement with our observations in the autologous NHP transplantation setting [11], robust multilineage engraftment of NHP cells in the PB of MISTRG mice was exclusively restricted to the sort-purified HSC-enriched cell fraction (I: CD90$^+$CD45RA$^-$), whereas no NHP cells were detected in mice injected with the MPP- (II) or LMP-enriched (III) cell fraction (Figure 3B). Upon necropsy, NHP multilineage engraftment in the BM, spleen, and thymus was only observed for mice transplanted with CD90$^+$CD45RA$^-$ cells (Figure 3C–F). HSC-enriched CD90$^+$CD45RA$^-$ cell fractions successfully gave rise to multilineage hematopoietic cells in the PB, BM, spleen, and thymus similar to previous experiments using bulk CD34$^+$ cells. Likewise, homing of CD34$^+$ cells and reconstitution of the BM HSPC compartment including all CD34 subsets was exclusively observed for mice receiving HSC-enriched cell fractions (Figure 3G). Most importantly, engrafted NHP CD34$^+$ cells maintained their differentiation potential giving rise to erythroid and myeloid colonies *ex vivo* (Figure 3H).

This data demonstrates that NHP CD90$^+$CD45RA$^-$ cells exclusively contain multipotent HSCs with multilineage engraftment and BM reconstitution potential.

NHP CD90$^+$CD45RA$^-$ cell fractions are enriched for multipotent HSCs

We have previously shown in the autologous NHP transplantation setting that the number of transplanted CD90$^+$CD45RA$^-$ cells correlates with the onset of neutrophil and platelet recovery and allows to predict successful long-term engraftment [11]; we have determined that a minimum of 122,000 CD90$^+$CD45RA$^-$ cells per kg bodyweight is required to prevent engraftment failure. To determine whether the xenograft potential of NHP cells recapitulates the autologous NHP transplant setting and to quantify the frequency of cells with mouse reconstitution potential, we next performed limiting dilution experiments of NHP CD34$^+$ HSPCs and CD90$^+$CD45RA$^-$ cell fractions.

Three different cell doses (10×10^4, 7.5×10^4 and 5×10^4) were transplanted into MISTRG mice and engraftment of NHP cells in the PB as well as other tissues analyzed as previously described (Table 3C). Robust multilineage engraftment of NHP cells in the PB and tissues

was observed in all mice transplanted with 1×10^5 $CD90^+CD45RA^-$ cells, whereas the chimerism was lower in animals receiving the same number of bulk $CD34^+$ cells (Figure 4A–C). NHP chimerism in both groups gradually decreased with lower number of cells injected, and the average frequency of NHP blood cells in all tissues was consistently higher in mice transplanted with $CD90^+CD45RA^-$ cells (Figure 4A–C). Similarly, greater engraftment of NHP $CD34^+$ cells, phenotypical CD34 subsets, as well as $CD34^+$ cells with CFC potential was seen in mice receiving $CD90^+CD45RA^-$ cells compared to bulk $CD34^+$ fractions (Figure 4D and E).

Limiting-dilution calculation [20] for both cell fractions determined that NHP $CD34^+$ cell fractions contained 1 SRC (SCID repopulating cell) in 131×10^3 (range $64–267 \times 10^3$) transplanted cells (Figure 5A,B). $CD90^+CD45RA^-$ HSPCs were enriched for SRCs compared to $CD34^+$ bulk cells, with an estimate of 1 in 72.2×10^3 cells (range $35–147 \times 10^3$) demonstrating MISTRG engraftment potential (Figure 5A and B).

In summary, $CD90^+CD45RA^-$ HSPCs are enriched for SRC potential and reliably engraft in MISTRG mice transplanting a minimum dose of 73×10^3 cells per mouse.

Discussion

In this study, we demonstrate for the first time successful high-level multilineage engraftment of NHP hematopoietic cells in the PB, spleen, thymus, and BM in a xenogeneic transplantation mouse model. This novel “monkeynized” MISTRG mouse model supports dose-dependent engraftment as well as multilineage differentiation of NHP blood cells, enables homing of NHP HSPCs into the BM stem cell niche, and supports complete reconstitution of phenotypically and functionally distinct NHP HSPC subpopulations. Most importantly, this mouse model recapitulates our recent findings obtained by autologous NHP transplantation, thus confirming exclusive enrichment of NHP stem and progenitor cells with multilineage engraftment potential in the $CD34^+CD90^+CD45RA^-$ phenotype.

The analysis of primary NHP HSPCs using the mouse xenograft model has rarely been performed in the last decades. One of the first studies reporting successful but low level engraftment (0.13–2%) of gene-modified and transplanted baboon HSPCs (2×10^6 cells per mouse) was reported in 2003 by Horn *et al.* using the NOD/SCID mouse model [12]. In their comprehensive side-by-side comparison of autologous transplantation in the baboon vs. the NOD/SCID xenograft model, Horn *et al.* observed lympho-myeloid engraftment of NHP cells in primary as well as secondary mice [12]. Despite this encouraging finding, there was a continuous decline in the level of engraftment over the course of 12 weeks in the mouse xenograft model, and we interpret this observation as indicating that NHP SRCs were most likely short-term repopulating cells rather than multipotent HSCs.

With this fairly limited frequency of chimerism, NHP xenograft assays have not been extensively used in the past years, and little effort has been spent on improving the existing model(s). However, with the discovery of induced pluripotent stem cells (IPSCs), the reprogramming of NHP fibroblasts/endothelial cells into IPSCs, and the overarching goal to differentiate NHP-IPSCs into functional HSPCs for regenerative medicine, the requirement

for a functional *in vivo* readout of NHP HSPCs is becoming evident again. By transplanting IPSC-derived HSPCs from the pigtail macaque [21] and cynomologus monkey (*Macaca fascicularis*) [22] into subleathally irradiated NSG mice, successful multilineage engraftment of up to 10% $CD45^+$ NHP cells has been observed in the PB of individual mice [21]. Most importantly, IPSC-derived NHP HSPCs homed into the murine BM stem cell compartment, gave rise to erythro-myeloid colonies *ex vivo*, and engrafted into secondary recipients [21]. While these findings are very encouraging, it remains unknown whether these IPSC-derived NHP HSPCs would be capable of long-term engraftment in an autologous transplant setting. Based on the observed incompatibility of NHP HSPCs in the NSG mouse model, we would expect that MISTRG mice could potentially demonstrate greatly enhanced support for NHP-IPSC derived HSPCs as well as mature blood cells.

Fueled by recent advances in HSC gene therapy/editing, the demand for *in vivo* models that are feasible for high-throughput screening of novel reagents (vectors, nucleases), delivery methods (AAV, nanoparticles), and target cell fractions is steadily increasing. Closely reflecting the homing and reconstitution of the BM stem cell compartment in the autologous setting, the monkeynized MISTRG mouse model offers a great opportunity to comprehensively test novel HSC gene therapy/editing therapies before performing long-lasting large animal studies and ultimately applying novel strategies to patients. The detection of NHP cells with a T cell-like phenotype may potentially enable us to test and pre-evaluate CAR T cells as well as HIV treatment strategies that are currently either tested *ex vivo* in T cell cultures or in expensive NHP studies [23]. Strategies including the knockout of CCR5 [7], the generation of anti-HIV CAR T cells [24, 25], or the development of broadly neutralizing anti-HIV antibodies [26] can be comprehensively tested in this novel model and inform large-animal studies. More detailed analysis will be required to evaluate the maturation and test the functionality of phenotypically distinct NHP T cell subsets (naïve, effector and memory) generated in this new mouse model.

The engraftment of NHP HSPCs in the BM stem cell compartment as well as the maturation of NHP B cells and T cells in the MISTRG mouse model is very likely attributed to the nearly entire (99.8%) conservation of the “dońt-eat-me” signal between humans and pigtail macaques (Supplementary Table E2). While this model promotes the differentiation of NHP HSPCs into phenotypically mature lymphocytes, the maturation of NHP granulocytes and monocytes seems to be less well supported due to potential incompatibility of essential cytokines. Despite high homology of human and NHP macrophage colony-stimulating factor (M-CSF, 99.4%) as well as granulocyte-macrophage colony-stimulating factor (GM-CSF, 99.3%), two cytokines required for terminal myeloid differentiation [27, 28], interleukin 3 (IL3) demonstrates only 82.1% similarity (Supplementary Table E2). IL3 is a critical factor in early hematopoiesis [29], synergistically acts with M-CSF as well as GM-CSF in myelopoiesis [30, 31], and therefore may be the main cause for the low level of myeloid NHP cells in MISTRG mice. Genetical engineering of MISTRG mice with NHP IL3 would potentially help to overcome this limitation and enable similar levels of NHP granulocytes and monocytes observed with human cells [14].

One of the most important findings is the nearly identical engraftment pattern of NHP HSPC subpopulations. Similar to our most recent report comparing phenotypically defined HSPC

subsets in competitive and autologous repopulation studies [11], the $CD34^+CD90^+CD45RA^-$ subset exclusively contained multilineage engraftment potential and the ability to reconstitute the BM stem cell compartment. In contrast to our autologous studies co-infusing sort-purified, cultured and *ex vivo* gene-modified subsets, engraftment studies of individual sort-purified HSPC subsets in the MISTRG mouse model suggest that the transplantation of $CD90^+CD45RA^-$ cells alone is sufficient and does not require the co-administration of downstream progenitor cells. However, limiting-dilution experiments indicate that the xenograft potential of purified $CD90^+CD45RA^-$ cells in MISTRG mice is increased when co-transplanted with downstream progenitors. It remains unknown at this point whether committed progenitors either support the BM homing of intravenously administered $CD90^+CD45RA^-$ cells or protect more primitive cells from exhaustion providing short-term recovery. Despite this open question, we here confirm that freshly-isolated and unmanipulated MPP- and LMP-enriched CD34 subsets alone are not capable to engraft in the analyzed tissues. The reproducibility of engraftment patterns observed in the autologous setting as well as comparable levels of chimerism with similar numbers of transplanted human and NHP $CD34^+$ cells further highlights the relevance of this mouse model for the pre-clinical development and high-throughput screening of novel HSC-mediated gene therapy/editing approaches.

When comparing the engraftment and multilineage development of non-human primate vs. human adult $CD34^+$ cells upon transplantation in MISTRG mice, we observed that both species yielded very similar results [32]. Chimerism reaches high levels (30–50%) as early as 8 weeks' post-transplantation; $CD34^+$ HSPCs, with an immunophenotype enriched for long-term HSCs ($CD90^+CD45RA^-$) are found in similar frequency; and multilineage differentiation, including B and T lymphocytes as well as myeloid cells is observed. However, non-human primate monocytosis appears to be defective; this may be due to insufficient cross-reactivity of human IL-3 on the monkey receptor. It is likely the transplantation of newborn monkey $CD34^+$ cells would more robustly engraft, as observed with human cord blood cells.

In summary, we here show a novel monkeynized mouse model that efficiently promotes the engraftment of NHP HSPCs and closely resembles the engraftment kinetics of NHP HSPC subsets observed in the autologous transplant setting. Availability of this novel NHP xenograft model has the potential to significantly reduce the costs for large-animal transplants, facilitate the high-throughput screening of gene therapy and potentially CAR T cell strategies *in vivo*, and enable a more objective selection of conditions that are ultimately tested and tracked long-term in the NHP.

Methods

Cell Sources and $CD34^+$ Enrichment

Nonhuman primate $CD34^+$ cells were harvested, enriched, and cultured as previously described [11, 33, 34]. Briefly, before enrichment of NHP $CD34^+$ cells, red cells were lysed in ammonium chloride lysis buffer, and WBCs were incubated for 20 minutes with the 12.8 immunoglobulin-M anti-CD34 antibody, then washed and incubated for another 20 minutes with magnetic-activated cell-sorting anti-immunoglobulin-M microbeads (Miltenyi Biotech,

Bergisch Gladbach, Germany). The cell suspension was run through magnetic columns enriching for $CD34^+$ cell fractions with a purity of 60% to 80% confirmed by flow cytometry.

Flow Cytometry Analysis and FACS

Antibodies used for flowcytometric analysis and FACS (fluorescence-activated cell sorting) of NHP and human cells are listed in Supplementary Table E2. Dead cells and debris were excluded via FSC/SSC gating. Flow cytometric analysis was performed on an LSR IIu (BD, Franklin Lakes, NJ), Fortessa X50 (BD) and FACSAria IIu (BD). Cells for *in vitro* assays were sorted using a FACSAria IIu cell sorter (BD).

Colony-Forming Cell (CFC) Assay

For CFC assays, 1000–1200 sort-purified NHP or CD34-subpopulations were seeded into 3.5 mL ColonyGEL 1402 (ReachBio, Seattle, WA). Hematopoietic colonies were scored after 12–14 days. Arising colonies were identified as colony-forming unit- (CFU-) granulocyte (CFU-G), macrophage (CFU-M), granulocyte-macrophage (CFU-GM), or burst-forming unit-erythrocyte (BFU-E). Colonies consisting of erythroid and myeloid cells were scored as CFU-MIX.

Mouse xenograft transplantation

Neonatal MISTRG mice (*CSF1*$^{h/h}$ *IL3/CSF2*$^{h/h}$*SIRPA*^{tg} *THPO*$^{h/h}$ *Rag2*$^{-/-}$ *Il2rg*$^{-/-}$) and NSG mice (NOD.Cg-*Prkdc*^{scid}*Il2rg*^{tm1Wjl}/SzJ) within 48–72 hours of birth, or adult (8–12 week) NSG mice received a radiation dose of 150 cGy (neonatal MISTRG/NSG) or 275 cGy (adult NSG) followed 4 hours later by a 200 μL intravenous injection of sort-purified NHP $CD34^+$ cells or CD34-subpopualtion. Beginning at 6–8 weeks post-injection, blood samples were collected biweekly and analyzed by flow cytometry for expression of human lineage markers (see Supplementary Table E2). After 16–24 weeks, animals were sacrificed, and tissues harvested and dissociated through 70 μm filters for analysis. All animal studies were carried out at Fred Hutchinson Cancer Research Center (Fred Hutch) in compliance with the approved IACUC protocol #1483.

Statistics

Data analysis of limiting dilution experiments was performed as previously described [20]. Statistical analysis of data was performed using GraphPad Prism Version 5. Significance analyses were performed with the unpaired, two-sided Student's t-test (*: $p < 0.05$; **: $p < 0.01$; ***: $p < 0.001$).

Supplementary Material

Refer to Web version on PubMed Central for supplementary material.

Acknowledgements

We thank Helen Crawford for help in preparing this manuscript. We acknowledge Yale University, the University of Zürich and Regeneron Pharmaceuticals where MISTRG mice were generated thanks to the financial support of the Bill and Melinda Gates Foundation.

Funding: This work was supported in part by grants to HPK from the National Institutes of Health, Bethesda, MD: HL115128, HL098489, AI096111 and by grants to AR the Bezos family (AR), the National Cancer Institute of the National Institutes of Health (T32 CA080416; TRS), and the Cooperative Center of Excellence in Hematology (U54 DK106829; AR). This research was also supported by Shared Resources (Comparative Medicine, Flow Cytometry and Experimental Histopathology) of the Fred Hutch/University of Washington Cancer Consortium (P30 CA015704). HPK is a Markey Molecular Medicine Investigator and received support as the inaugural recipient of the José Carreras/E. Donnall Thomas Endowed Chair for Cancer Research and the Fred Hutch Endowed Chair for Cell and Gene Therapy.

References

[1]. Adair JE, Kubek SP, Kiem HP. Hematopoietic Stem Cell Approaches to Cancer. Hematol Oncol Clin North Am. 2017;31:897–912. [PubMed: 28895855]

[2]. Morgan RA, Gray D, Lomova A, Kohn DB. Hematopoietic stem cell gene therapy: Progress and lessons learned. Cell Stem Cell. 2017;21:574–590. [PubMed: 29100011]

[3]. Tran E, Longo DL, Urba WJ. A Milestone for CAR T Cells. N Engl J Med. 2017;377:2593–2596. [PubMed: 29226781]

[4]. D'Aloia MM, Zizzari IG, Sacchetti B, Pierelli L, Alimandi M. CAR-T cells: the long and winding road to solid tumors. Cell death & disease. 2018;9:282. [PubMed: 29449531]

[5]. Becker PS, Taylor JA, Trobridge GD, et al. Preclinical correction of human Fanconi anemia complementation group A bone marrow cells using a safety-modified lentiviral vector. Gene therapy. 2010;17:1244–1252. [PubMed: 20485382]

[6]. Burtner CR, Beard BC, Kennedy DR, et al. Intravenous injection of a foamy virus vector to correct canine SCID-X1. Blood. 2014;123:3578–3584. [PubMed: 24642749]

[7]. Peterson CW, Wang J, Norman KK, et al. Long-term multi-lineage engraftment of genome-edited hematopoietic stem cells after autologous transplantation in nonhuman primates. Blood. 2016.

[8]. Humbert O, Peterson CW, Norgaard ZK, Radtke S, Kiem HP. A nonhuman primate transplantation model to evaluate hematopoietic stem cell gene editing strategies for beta-hemoglobinopathies. Mol Ther Methods Clin Dev. 2018;8:75–86. [PubMed: 29276718]

[9]. Trobridge GD, Kiem HP. Large animal models of hematopoietic stem cell gene therapy. Gene therapy. 2010;17:939–948. [PubMed: 20428209]

[10]. Larochelle A, Dunbar CE. Genetic manipulation of hematopoietic stem cells. Seminars in hematology. 2004;41:257–271. [PubMed: 15508111]

[11]. Radtke S, Adair JE, Giese MA, et al. A distinct hematopoietic stem cell population for rapid multilineage engraftment in nonhuman primates. Science translational medicine. 2017;9.

[12]. Horn PA, Thomasson BM, Wood BL, Andrews RG, Morris JC, Kiem HP. Distinct hematopoietic stem/progenitor cell populations are responsible for repopulating NOD/SCID mice compared with nonhuman primates. Blood. 2003;102:4329–4335. [PubMed: 12816869]

[13]. Ishikawa F, Yasukawa M, Lyons B, et al. Development of functional human blood and immune systems in NOD/SCID/IL2 receptor {gamma} chain(null) mice. Blood. 2005;106:1565–1573. [PubMed: 15920010]

[14]. Rongvaux A, Willinger T, Martinek J, et al. Development and function of human innate immune cells in a humanized mouse model. Nat Biotechnol. 2014;32:364–372. [PubMed: 24633240]

[15]. Ishikawa F Modeling normal and malignant human hematopoiesis in vivo through newborn NSG xenotransplantation. Int J Hematol. 2013;98:634–640. [PubMed: 24258713]

[16]. Barclay AN, Van den Berg TK. The interaction between signal regulatory protein alpha (SIRPalpha) and CD47: structure, function, and therapeutic target. Annu Rev Immunol. 2014;32:25–50. [PubMed: 24215318]

[17]. Takenaka K, Prasolava TK, Wang JC, et al. Polymorphism in Sirpa modulates engraftment of human hematopoietic stem cells. Nat Immunol. 2007;8:1313–1323. [PubMed: 17982459]

[18]. Herndler-Brandstetter D, Shan L, Yao Y, et al. Humanized mouse model supports development, function, and tissue residency of human natural killer cells. Proc Natl Acad Sci U S A. 2017;114:E9626–E9634. [PubMed: 29078283]

[19]. Deng K, Pertea M, Rongvaux A, et al. Broad CTL response is required to clear latent HIV-1 due to dominance of escape mutations. Nature. 2015;517:381–385. [PubMed: 25561180]

[20]. Hu Y, Smyth GK. ELDA: extreme limiting dilution analysis for comparing depleted and enriched populations in stem cell and other assays. Journal of immunological methods. 2009;347:70–78. [PubMed: 19567251]

[21]. Gori JL, Chandrasekaran D, Kowalski JP, et al. Efficient generation, purification, and expansion of CD34(+) hematopoietic progenitor cells from nonhuman primate-induced pluripotent stem cells. Blood. 2012;120:e35–44. [PubMed: 22898598]

[22]. Abed S, Tubsuwan A, Chaichompoo P, et al. Transplantation of Macaca cynomolgus iPS-derived hematopoietic cells in NSG immunodeficient mice. Haematologica. 2015;100:e428–431. [PubMed: 26088930]

[23]. Peterson CW, Haworth KG, Burke BP, et al. Multilineage polyclonal engraftment of Cal-1 gene-modified cells and in vivo selection after SHIV infection in a nonhuman primate model of AIDS. Mol Ther Methods Clin Dev. 2016;3:16007. [PubMed: 26958575]

[24]. Zhen A, Peterson CW, Carrillo MA, et al. Correction: Long-term persistence and function of hematopoietic stem cell-derived chimeric antigen receptor T cells in a nonhuman primate model of HIV/AIDS. PLoS pathogens. 2018;14:e1006891. [PubMed: 29529058]

[25]. Kuhlmann AS, Peterson CW, Kiem HP. Chimeric antigen receptor T-cell approaches to HIV cure. Curr Opin HIV AIDS. 2018.

[26]. Wibmer CK, Moore PL, Morris L. HIV broadly neutralizing antibody targets. Current opinion in HIV and AIDS. 2015;10:135–143. [PubMed: 25760932]

[27]. Clark SC, Kamen R. The human hematopoietic colony-stimulating factors. Science. 1987;236:1229–1237. [PubMed: 3296190]

[28]. Sieff CA. Hematopoietic growth factors. The Journal of clinical investigation. 1987;79:1549–1557. [PubMed: 3034976]

[29]. Robin C, Ottersbach K, Durand C, et al. An unexpected role for IL-3 in the embryonic development of hematopoietic stem cells. Developmental cell. 2006;11:171–180. [PubMed: 16890157]

[30]. Donahue RE, Seehra J, Metzger M, et al. Human IL-3 and GM-CSF act synergistically in stimulating hematopoiesis in primates. Science. 1988;241:1820–1823. [PubMed: 3051378]

[31]. Lachmann N, Ackermann M, Frenzel E, et al. Large-scale hematopoietic differentiation of human induced pluripotent stem cells provides granulocytes or macrophages for cell replacement therapies. Stem cell reports. 2015;4:282–296. [PubMed: 25680479]

[32]. Saito Y, Ellegast JM, Rafiei A, et al. Peripheral blood CD34(+) cells efficiently engraft human cytokine knock-in mice. Blood. 2016;128:1829–1833. [PubMed: 27543436]

[33]. Trobridge GD, Beard BC, Gooch C, et al. Efficient transduction of pigtailed macaque hematopoietic repopulating cells with HIV-based lentiviral vectors. Blood. 2008;111:5537–5543. [PubMed: 18388180]

[34]. Adair JE, Waters T, Haworth KG, et al. Semi-automated closed system manufacturing of lentivirus gene-modified haematopoietic stem cells for gene therapy. Nat Commun. 2016;7:13173. [PubMed: 27762266]

Highlights

1. MISTRG mice support engraftment of NHP hematopoietic stem and progenitor cells
2. MISTRG engraftment is exclusively restricted to NHP $CD34^{+}CD90^{+}CD45RA^{-}$ cells
3. Engraftment in MISTRG recapitulates reconstitution in autologous NHP transplants

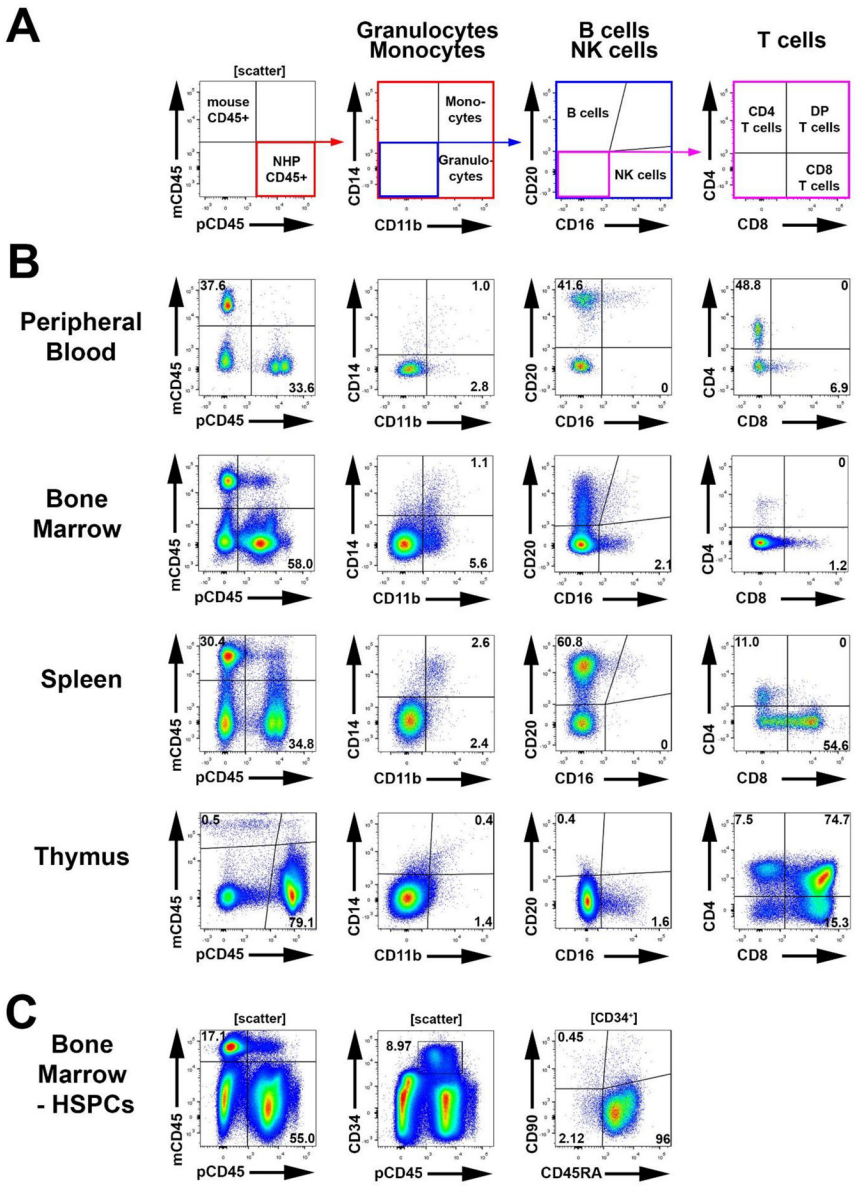

Figure 1: Multilineage engraftment of NHP cells in the MISTRG mouse model.

(A) Gating strategy for the flow-cytometric assessment of NHP CD45$^+$ cells (pCD45, 1st plot), granulocytes (CD11b$^+$CD14$^-$) vs. monocytes (CD11b$^+$CD14$^+$) (2nd plot), B cells (CD20$^+$) vs. NK cells (CD16$^+$) (3rd plot), and different T cell subsets (CD3$^+$/CD4$^+$/CD8$^+$) (4th and 5th plot). **(B)** Representative gating for the assessment of NHP lineage subsets in the BM, PB, spleen and thymus of successfully engrafted MISTRG mice. **(C)** Representative gating strategy for the assessment and quantification of engrafted NHP CD34$^+$ HSPC subpopulations in the BM of MISTRG mice.

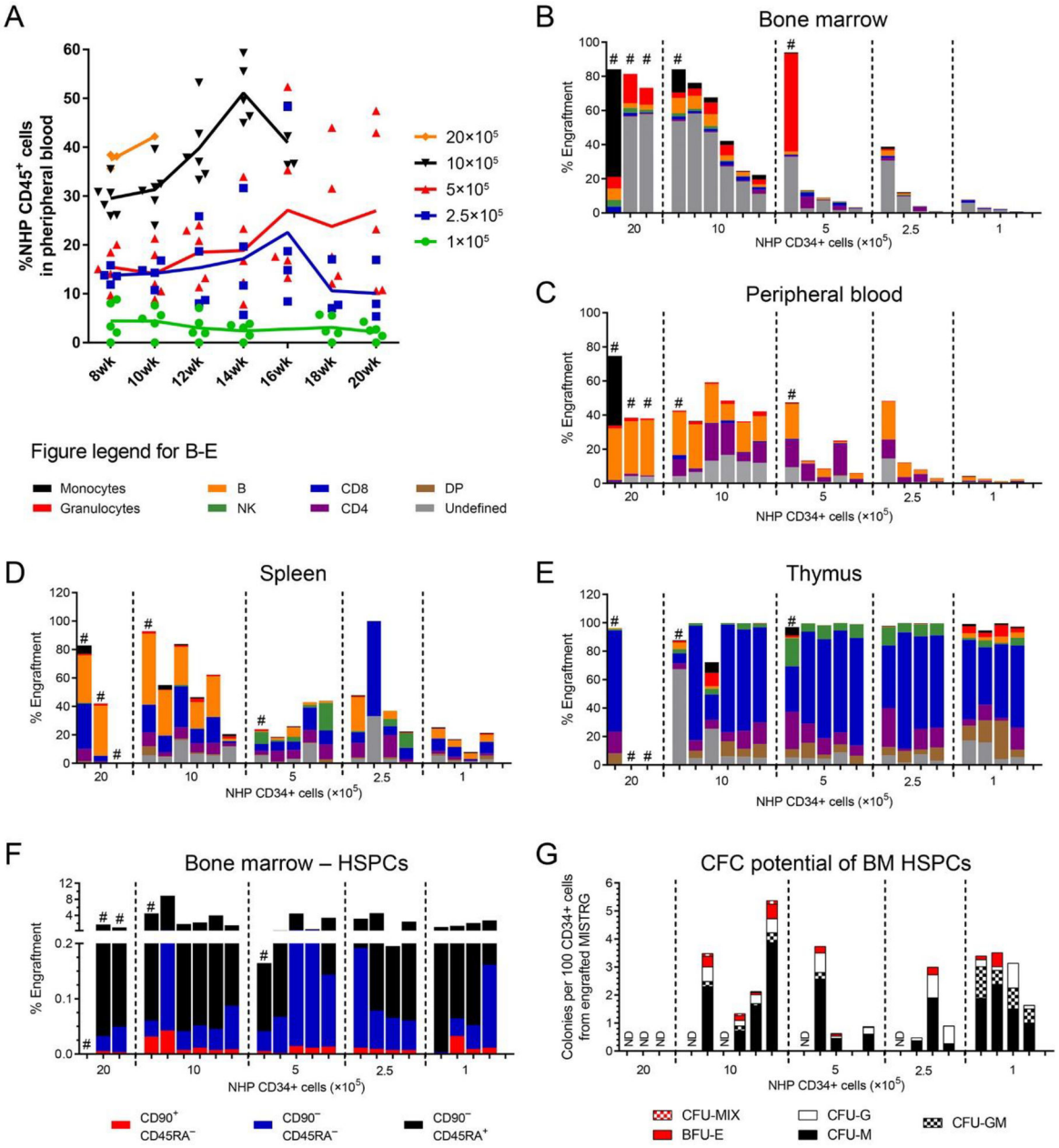

Figure 2: Multilineage engraftment of NHP CD34$^+$ HSPCs in the MISTRG mouse model

(A) Longitudinal tracking of NHP CD45$^+$ cells in the peripheral blood of MISTRG mice after sub-lethal irradiation and transplantation of NHP CD34$^+$ HSPCs in different quantities as indicated in the figure legend. **(B-E)** Frequency of NHP monocytes (CD11b$^+$CD14$^+$), granulocytes (CD11b$^+$CD14$^-$), B cells (CD20$^+$), NK cells (CD16$^+$) and T cells (CD4$^+$/CD8$^+$/CD4$^+$CD8$^+$) in the (B) BM, (C) PB, (D) spleen and (E) thymus 16–20 weeks after transplant. Mice in all graphs and within each group are organized from the highest to the lowest engraftment level in the BM. **(F)** Frequency of NHP CD34$^+$ cells (total height of bars) and CD34$^+$ subpopulations (color-coded) within BM-resident NHP CD45$^+$ cells. **(G)** Erythroid, myeloid and erythro-myeloid colony-forming potential of engrafted NHP CD34$^+$

cells. $CD34^+$ cells were sort-purified, introduced into CFC assays, and different colony-subtypes (color-coded) quantified after 14 days. (DP = $CD4^+CD8^+$ double-positive T cells; ND = not determined, # = mice were subject to early euthanasia due to severe weight loss or anemia)

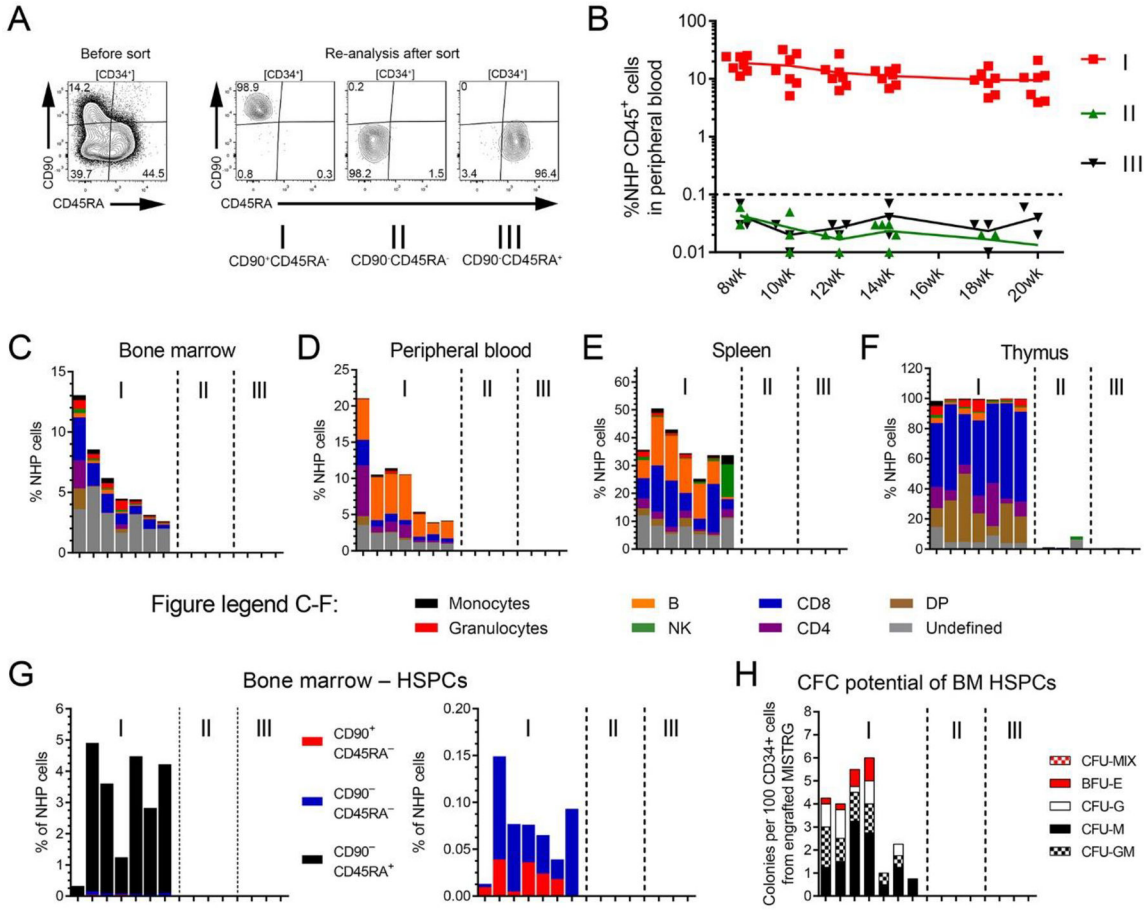

Figure 3: Engraftment potential of freshly-isolated NHP CD34-subpopulations in MISTRG mice

(A) Gating and sorting strategy for transplanted HSC- (I: $CD90^{+}CD45RA^{-}$), MPP- (II: $CD90^{-}CD45RA^{-}$) and LMP- (III: $CD90^{-}CD45RA^{+}$) enriched NHP CD34-subpopulations. **(B)** Frequency of NHP $CD45^{+}$ cells in the PB of transplanted mice over time. **(C-F)** Multilineage engraftment of NHP blood lineages in the (C) BM, (D) PB, (E) spleen and (F) thymus 20 weeks post-transplant. Mice in all graphs and within each group are organized from the highest to the lowest engraftment level in the BM. **(G)** Frequency of NHP $CD34^{+}$ cells (total height of bars) and $CD34^{+}$ subpopulations (color-coded) within BM-resident NHP $CD45^{+}$ cells. **(H)** Erythroid, myeloid and erythro-myeloid colony-forming potential of engrafted NHP $CD34^{+}$ cells.

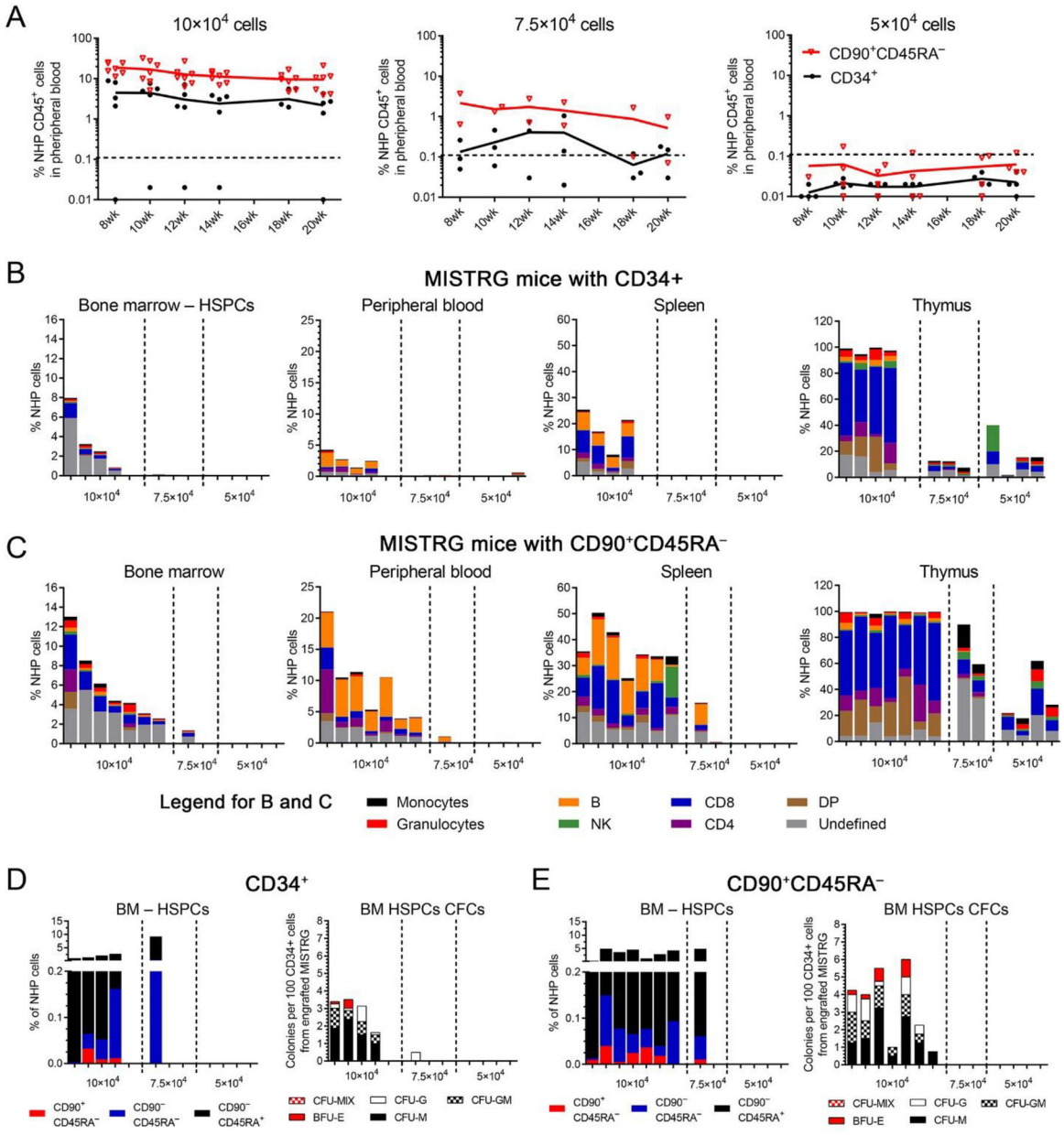

Figure 4: Limiting dilution experiments of NHP CD34$^+$ and CD90$^+$CD45RA$^-$ cell fractions

(A) Frequency of NHP CD45$^+$ cells in the PB of transplanted mice over time after infusion of CD34$^+$ cells or CD90$^+$CD45RA$^-$ cell fractions in different quantities. **(B+C)** Multilineage engraftment of NHP blood lineages in the BM, PB, spleen and thymus 20 weeks' post-transplant and infusion of (B) CD34$^+$ cells or (C) CD90$^+$CD45RA$^-$ cell fractions. **(D+E, left graph)** Frequency of NHP CD34$^+$ cells (total height of bars) and CD34$^+$ subpopulations (color-coded) within BM-resident NHP CD45$^+$ cells. **(D+E, right graph)** Erythroid, myeloid and erythro-myeloid colony-forming potential of engrafted NHP CD34$^+$ cells. CD34$^+$ cells were sort-purified, introduced into CFC assays, and different colony-subtypes (color-coded) quantified after 14 days. (DP = CD4$^+$CD8$^+$ double-positive T cells)

A

Bone marrow

×10⁴	CD34⁺	CD90⁺ CD45RA⁻
25	4/4	—
10	4/5	7/7
7.5	0/3	1/2
5	0/4	0/4

B

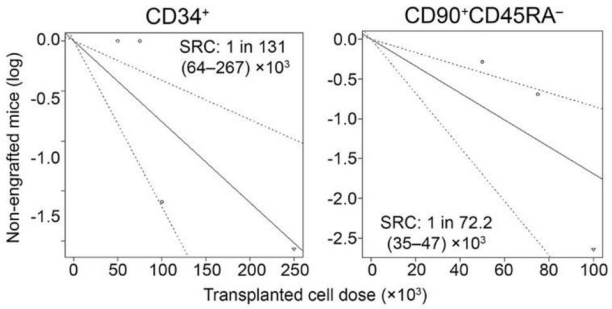

Figure 5: Calculation of SRCs in NHP CD34$^+$ and CD90$^+$CD45RA$^-$ cell fractions.

(A) Number of engrafted mice showing >0.1% NHP CD45$^+$ cells in the BM after transplanting limiting dilutions of NHP CD34$^+$ and CD90$^+$CD45RA$^-$ cell fractions. **(B)** Calculation of SRCs in NHP CD34$^+$ and CD90$^+$CD45RA$^-$ cell fractions.

Table 1.

Engraftment of NHP HSPCs in NSG mice

A	PM – 1 × 10^5 Primed BM	Adult NSG		Neonatal NSG	
		PB	BM	PB	BM
	$CD90^-CD45RA^+$	0/6	0/6	0/9	0/9
	$CD90^{+/-}CD45RA^-$	0/8	0/8	—	—
	$CD90^-CD45RA^-$	0/4	0/4	0/7	0/7
	$CD90^+CD45RA^-$	1/6	0/6	0/10	0/10

B	PM - $CD34^+$ Primed BM	Adult NSG		Neonatal NSG	
		PB	BM	PB	BM
	<1 × 10^4	0/2	0/2	—	—
	5-10 × 10^4	0/8	0/8	—	—
	10-15 × 10^4	0/6	0/6	0/6	0/6
	20-25 × 10^4	0/2	0/2	0/4	0/4
	50-75 × 10^4	0/2	0/2	0/3	0/3
	1 × 10^6	0/4	0/4	—	—

C	$CD34^+$ 5 × 10^5 - Adult NSG	Pigtail Macaque		Rhesus Macaque	
		PB	BM	PB	BM
	Primed BM	0/4	0/4	0/4	0/4
	Steady state BM	0/4	0/4	0/2	0/2

Freshly isolated and sort-purified NHP HSPCs were injected intravenously into NSG mice via the tail vein (adult mice) or intra-hepatic (neonatal mice) after sub-lethal irradiation (adult: 250 cGy; neonatal: 150 cGy). PB draws were performed every other week and the terminal endpoint for tissue harvest was performed 16–20 weeks' post-transplant. Mice were counted as engrafted when showing a distinct population of NHP $CD45^+$ cells >0.1% by flow-cytometry.

Table 2.

Cross-species conservation of amino acid sequences

[% Homology]	Mouse->Human	Mouse->Pigtail	Human->Pigtail
SIRPα	66.5%	67.8%*	91.9%*
CD47	70.3%	70.3%	99.8%
IL3	32.1%	32.9%	82.1%
M-CSF	69.9%	69.4%	99.4%
GM-CSF	54.9%	53.5%	99.3%
TPO	74.3%	73.9%	95.1%

Categories: red < 50%; yellow 50–90%; green > 90%.

*Rhesus Mulatta (Macaca nemestrina sequence not available)

Table 3.

Engraftment of NHP HSPCs in MISTRG mice

A PM - CD34$^+$	Neonatal MISTRG	
	PB	BM
25 × 10^4	7/7	6/7
50 × 10^4	9/9	9/9
100 × 10^4	6/6	6/6
200 × 10^4	3/3	3/3
B PM - CD34 Subpopulations		
CD90$^-$CD45RA$^+$	0/9	0/9
CD90$^-$CD45RA$^-$	0/17	0/17
CD90$^+$CD45RA$^-$	11/15	11/15
C Limiting Dilution		
CD34$^+$		
5 × 10^4	0/4	0/4
7.5 × 10^4	0/3	0/3
10 × 10^4	4/5	3/5
25 × 10^4	7/7	6/7
CD90$^+$		
5 × 10^4	0/4	0/4
7.5 × 10^4	1/2	1/2
10 × 10^4	7/7	7/7
25 × 10^4	—	—

Freshly isolated and sort-purified NHP HSPCs were injected intrahepatic into neonatal MISTRG mice after sub-lethal irradiation (150 cGy). PB draws were performed every other week and the terminal endpoint for tissue harvest was performed 16–20 weeks post-transplant. Mice were counted as engrafted when showing a distinct population of NHP CD45$^+$ cells >0.1% by flow-cytometry.